HHS Public Access

Author manuscript

Circ Res. Author manuscript; available in PMC 2021 November 06.

Published in final edited form as:

Circ Res. 2020 November 06; 127(11): 1347–1361. doi:10.1161/CIRCRESAHA.120.317175.

ILRUN, a Human Plasma Lipid GWAS Locus, Regulates Lipoprotein Metabolism in Mice

Xin Bi[1,4], **Takashi Kuwano**[1], **Paul C. Lee**[1], **John S. Millar**[1], **Li Li**[2], **Yachen Shen**[3], **Raymond E. Soccio**[3], **Nicholas J. Hand**[4], **Daniel J. Rader**[1,4,5]

[1]Division of Translational Medicine and Human Genetics, Department of Medicine; University of Pennsylvania, Philadelphia, PA 19104, USA.

[2]Penn Cardiovascular Institute; University of Pennsylvania, Philadelphia, PA 19104, USA.

[3]Department of Medicine; University of Pennsylvania, Philadelphia, PA 19104, USA.

[4]Department of Genetics; University of Pennsylvania, Philadelphia, PA 19104, USA.

[5]Department of Pediatrics, Perelman School of Medicine, University of Pennsylvania, Philadelphia, PA 19104, USA.

Abstract

Rationale: Single nucleotide polymorphisms (SNPs) near the *ILRUN* gene are genome-wide significantly associated with plasma lipid traits and coronary artery disease (CAD) but the biological basis of this association is unknown.

Objective: To investigate the role of ILRUN in plasma lipid and lipoprotein metabolism.

Methods and Results: *ILRUN* encodes a protein that contains a ubiquitin-associated (UBA)-like domain, suggesting that it may interact with ubiquitinylated proteins. We generated mice globally deficient for *Ilrun* (*Ilrun*KO) and found they had significantly lower plasma cholesterol levels resulting from reduced liver lipoprotein production. Liver transcriptome analysis uncovered altered transcription of genes downstream of lipid-related transcription factors, particularly PPARα, and livers from *Ilrun*KO mice had increased PPARα protein. Human ILRUN was shown to bind to ubiquitinylated proteins including PPARα, and the UBA-like domain of ILRUN was found to be required for its interaction with PPARα.

Conclusions: These findings establish ILRUN as a novel regulator of lipid metabolism that promotes hepatic lipoprotein production. Our results also provide functional evidence that *ILRUN*

Address correspondence to: Dr. Daniel J. Rader, University of Pennsylvania, 11-125 Smilow Center for Translational Research, 3400 Civic Center Blvd, Philadelphia, PA, 19104-5158, rader@pennmedicine.upenn.edu, Dr. Xin Bi, University of Pennsylvania, 11-165 Smilow Center for Translational Research, 3400 Civic Center Blvd, Philadelphia, PA, 19104-5158, xbi@pennmedicine.upenn.edu.

DISCLOSURES

None

SUPPLEMENTAL MATERIALS

Detailed Methods

Online Figures I–VIII

Online Table I–II

Major Resources Table

may be the casual gene underlying the observed genetic associations with plasma lipids at 6p21 in human.

Graphical Abstract

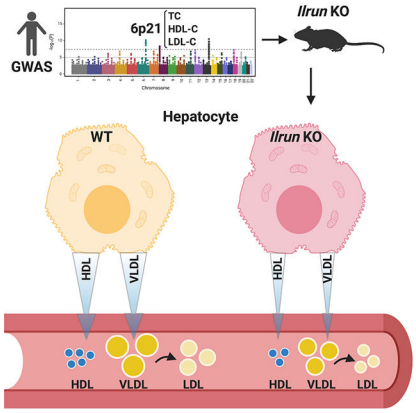

Keywords

Lipid and lipoprotein metabolism; ILRUN; hepatocyte; high-density lipoprotein cholesterol; low-density lipoprotein cholesterol

Subject Terms:

Basic Science Research; Lipids and Cholesterol; Metabolism

INTRODUCTION

Common population-level natural genetic variation with small effect sizes can reveal pathways and targets modulating plasma lipid levels with profound biological and clinical importance. Unbiased genome-wide association studies (GWAS) with follow-up functional validation studies therefore provide the opportunity to identify novel players in regulation of lipid metabolism and cardiovascular disease (CVD) risk[1–4]. GWAS for plasma lipid traits have identified over 300 independent genetic loci associated with at least one major plasma lipid trait, many of which have never been previously linked to lipid metabolism[5–14]. One compelling novel locus identified in early lipid GWAS is at chromosome 6p21, where multiple variants are genome-wide significantly associated with plasma total cholesterol (TC), high-density lipoprotein cholesterol (HDL-C), low-density lipoprotein cholesterol (LDL-C) levels, as well as with coronary artery disease (CAD)[15–17]. The lead SNPs at 6p21 are located either in the introns or within 9kb downstream of the gene, previously known as chromosome 6 open reading frame 106 (*C6ORF106*), which encodes an uncharacterized protein with no known relationship to lipid metabolism.

Other than a recent connection to antiviral immunity and cytokine production[18, 19], the biological function(s) of the protein encoded by *C6ORF106* remain largely unknown. One hint to its potential molecular functions comes from its two regions of sequence conservation, an N-terminal α-helical ‘ubiquitin associated domain-like’ (UBA-like) domain

and a ‘next to BRCA1 gene 1 protein’ (NBR1)-like domain[20, 21]. Members of the UBA-like domain superfamily have been implicated in various cellular processes, including binding of ubiquitinylated proteins, promotion of proteasomal degradation, and autophagy[22, 23]. The NBR1-like domain was named after a receptor for autophagosomal degradation of ubiquitinylated substrates[24–26]. While its function has yet to be fully characterized, the NBR1-like domain in ILRUN, together with the UBA-like domain, has recently been shown to be necessary for regulation of IRF3-DNA binding and downstream gene transcription in HeLa cells[19]. The mouse homologue of the C6ORF106 protein, D17wsu92e, shares significant sequence homology with and exhibits the same domain features as C6ORF106[20, 27]. The presence of these sequence motifs suggests a potential role for C6ORF106 in interacting with and regulating turnover of ubiquitinylated protein(s). Based on its sequence motifs, on published work[18], and on the data presented here, *C6ORF106* has been officially designated *ILRUN* (**I**nflammation and **L**ipid **R**egulator with **U**BA-like and **N**BR1-like domains). Our studies in mice demonstrate that ILRUN influences lipoprotein metabolism likely through modulation of lipid-related transcriptional regulators, particularly PPARα, identifying a novel functional role for this protein and helping to explain the relationship of genetic variation at this locus with plasma lipid traits.

METHODS

A Detailed Methods section is available in the Supplemental Materials. Please see the Major Resources Table in the Supplemental Materials. All animal experiment protocols and procedures were reviewed and approved by the Institutional Animal Care and Use Committees of the University of Pennsylvania.

Data Availability.

The majority of supporting data are presented within this article and its Data Supplement. Data that are not directly available are available from the corresponding author upon reasonable request. Microarray datasets have been deposited at Gene Expression Omnibus (GSE156151).

RESULTS

Generation of whole body IlrunKO mice and characterization of Ilrun expression.

Human *ILRUN* is ubiquitously expressed at variable levels across tissues, including in the liver[28]. To determine whether mouse *Ilrun* has a similar expression pattern, we examined *Ilrun* mRNA expression in an array of murine tissues from C57BL/6 wild-type (WT) mice. Indeed, expression of *Ilrun* varied greatly among tissues, with the highest level in skeletal muscle, modest expression in liver, and the lowest levels in pancreas (Figure 1A). To explore the impact of ILRUN on plasma lipid metabolism *in vivo*, we generated a global *Ilrun* knockout mouse model made using a gene trap strategy. The gene trap cassette consisting of a splice acceptor site, followed by a promoterless *lacZ* and neomycin-resistance fusion reporter gene was inserted into intron 1 of the *Ilrun* gene, which resulted in a truncated nonfunctional protein (Figure 1B). The presence of *lacZ* gene in the trapping cassette enables detection of active ILRUN expression by X-gal staining. Consistent with the mRNA

expression pattern in control mice, multiple tissues from *Ilrun*KO mice, including skeletal muscle, heart, liver, and aorta, were positively stained with X-gal (Figure 1C). Of interest, despite low mRNA expression levels, pancreatic ILRUN is specifically present in islets as shown by X-gal staining. Efficient *Ilrun* deletion was also validated at both the transcript and protein levels (Figure 1D and 1E). *Ilrun*KO mice are viable and fertile with no overt physical or behavioral abnormalities.

Ilrun regulates plasma lipid homeostasis in mice.

To investigate whether ILRUN plays a role in lipid metabolism *in vivo*, we characterized plasma lipid profiles of *Ilrun*KO and control mice (Online Table I). When mice were maintained on chow diet, plasma TC levels in 4h-fasted *Ilrun*KO versus WT mice were consistently and significantly lower (Figure 2A), largely attributable to decreased HDL-C levels (Figure 2B and 2C) consistent with the fact that HDL-C is a major contributor to TC in chow-fed C57BL/6 mice. A proportional reduction in phospholipids (PL) was also seen in *Ilrun*KO relative to control mice, whereas no significant differences in TG or non-esterified fatty acids (NEFA) were found between groups (Online Figure IA). Fast protein liquid chromatography (FPLC) analysis of lipoprotein distribution confirmed the predominant decrease in HDL associated cholesterol in *Ilrun*KO mice and lack of significant differences in TGs between groups (Figure 2D and Online Figure IA). To further study the effects of *Ilrun* on lipoprotein metabolism, mice were fed a western type diet (WTD) for 14wks. While plasma cholesterol levels increased for both groups of mice with WTD consumption, the response was attenuated in *Ilrun*KO mice, leading to significantly reduced TC, HDL-C, non-HDL-C (Figure 2E–G), and PL (Online Figure IB) levels over time. TC in fractions representing LDL and HDL particles, especially relatively small LDL and large HDL, was markedly reduced (Figure 2H and Online Figure IB). Similar to chow-fed mice, plasma TG level and distribution did not differ between genotypes (Online Figure IB). Changes in plasma cholesterol homeostasis in the absence of *Ilrun* could be a result of altered intestinal absorption, hepatic lipoprotein production, or tissue uptake and biliary excretion[29]. No differences in the body weight or weights of tissues, including liver and adipose tissues (white, brown, and subcutaneous), were found in mice maintained on chow diet at various ages (Online Figure IC). When challenged with WTD, *Ilrun*KO mice had significantly lower body weight towards the end of the study that coincided with decreased liver to body weight ratio in these mice (Online Figure ID). Additionally, similar fractional cholesterol absorption, food intake, and fecal neutral sterol excretion were observed between genotypes of mice (Online Figure IE–G). Hence, impaired intestinal absorption or increased fecal excretion is not likely the primary explanation for the lower plasma cholesterol in *Ilrun*KO mice.

Ilrun regulates lipoprotein metabolism in a liver dependent manner.

To test whether ILRUN expression in liver, a central regulator of lipoprotein metabolism, mediates the lipid-regulatory effects of ILRUN, we expressed the human *ILRUN* cDNA specifically in the livers of the *Ilrun*KO mice using an adeno-associated virus serotype 8 (AAV8) vector under the control of a thyroxine binding globulin (TBG) hepatocyte-specific promoter. Groups of chow-fed WT control and *Ilrun*KO mice were injected with either a control empty AAV8 vector (AAV-null) or an AAV8 vector expressing *ILRUN* (AAV-

ILRUN). Deletion of endogenous murine *Ilrun* and expression of reconstituted human *ILRUN* were confirmed at both transcript and protein levels (Online Figure IIA–B). In concordance with previous findings in chow diet studies, *Ilrun*KO mice displayed a ~30% reduction in TC, HDL-C, and PL levels relative to control mice at baseline before injection (0wk). As expected, introduction of AAV-null into livers did not change these differences between WT and *Ilrun*KO mice. In contrast, human *ILRUN* reconstitution in *Ilrun*KO livers completely restored plasma TC (83 ± 4 mg/dl in WT-AAV-null vs. 86 ± 2 mg/dl in *Ilrun*KO-AAV-*ILRUN*; Figure 3A), HDL-C (62 ± 3 mg/dl in WT-AAV-null vs. 65 ± 2 mg/dl in *Ilrun*KO-AAV-*ILRUN*; Figure 3B) and PL (172 ± 7 mg/dl in WT-AAV-null vs. 169 ± 7 mg/dl in *Ilrun*KO-AAV-*ILRUN*; Online Figure IIC) to those of WT mice levels as early as 2 wks after injection, and maintained the effect until the end of the study (4.5wk). This effect of *ILRUN* reconstitution was further evidenced by normalization of TC (Figure 3C and 3D) and PL (Online Figure IID–E) distribution in small LDL and HDL regions based on FPLC analysis. Overall, these data demonstrate that ILRUN regulates plasma lipid metabolism *in vivo*, impacting both HDL and non-HDL lipoprotein metabolism and that this phenotype primarily reflects the effects of hepatocyte-expressed ILRUN. This supports the notion that *ILRUN* is likely the causal gene responsible for the genetic association of genetic variants with lipid traits at the human 6p21 locus.

Deletion of Ilrun lowers plasma HDL-C by reducing HDL production.

To elucidate the metabolic pathway(s) through which ILRUN modulates plasma HDL-C levels, we tested the hypothesis that hepatic ILRUN deletion reduces HDL-C levels by increasing HDL catabolism. HDLs were radiolabeled with ^{3}H-cholesteryl ether and ^{125}I-tyramine cellobiose[30] for i.v. injection into chow-fed mice. The fate of these dual radiolabeled HDL particles was then traced over the course of 24 hours after injection. Plasma decay of ^{125}I-labeled apoA-I (Online Figure IIIA) and ^{3}H labeled cholesterol (Online Figure IIIB) was indistinguishable between groups, leading to comparable fractional catabolic rate (FCR) of plasma ^{125}I (Online Figure IIIC) and ^{3}H (Online Figure IIID). Scavenger receptor class B1 (SR-BI) mediated HDL selective uptake[31] was also similar between genotypes (Online Figure IIIE). No significant difference in FCR of HDL CE or HDL protein over the course of 24 hours was found in WTD-fed mice (data not shown). Together, these data showed that the absence of ILRUN had no major impact on HDL catabolism, and suggested that attenuated hepatic HDL production is likely the underlying mechanism for lower HDL-C in *Ilrun*KO mice.

Consistent with this concept, a significant decrease in mRNA and protein expression of apoA-I, a main protein constituent of HDL particles that is critical for HDL formation, was found in primary hepatocytes from *Ilrun*KO vs. control mice (Figure 4A–B). Total plasma apoA-I (Figure 4C) and apoA-I levels in HDL fractions of plasma from chow-fed *Ilrun*KO mice (Figure 4D) were also reduced. Similarly, liver apoA-I protein expression in WTD-fed *Ilrun*KO vs. WT mice was noticeably lower (Figure 4E), which is in line with decreased apoA-I associated with HDL particles of different sizes when *Ilrun* was absent (Figure 4F). In addition, chow-fed *Ilrun*KO mice had ~32% reduced liver apoA-I protein expression that was restored with hepatic *ILRUN* expression, while SR-BI and ABCA1 protein levels stayed the same among groups (Online Figure IIB and IIF). These results strongly support that loss

of *Ilrun* lowers plasma HDL-C by attenuating hepatic apoA-I production and subsequent HDL formation.

Deletion of Ilrun decreases VLDL-TG secretion.

*Ilrun*KO mice also exhibited lower non-HDL-C levels, which was most pronounced in mice in which apolipoprotein B containing lipoprotein (apoBLp) levels were raised by WTD feeding. The liver regulates non-HDL-C levels through secretion of very low-density lipoproteins (VLDL), the precursor of LDL, and through clearance of apoBLp. We performed *in vivo* VLDL-TG and apoB secretion studies to test whether decreased VLDL secretion accounts for the lower non-HDL-C in *Ilrun*KO mice. Poloxamer 407 and ^{35}S-methionine/cysteine were injected into WTD-fed mice to inhibit lipoprotein lipase (LPL) and label newly synthesized proteins respectively. As expected, plasma TG levels dramatically increased in WT mice during the course of 4 hours. However, the accumulation of plasma TG in response to LPL inhibition was attenuated in *Ilrun*KO mice (Figure 5A), resulting in a ~32% reduction in VLDL-TG secretion rate compared to that of control mice (Figure 5B). In parallel, we compared the secretion of newly synthesized apoB100 and apoB48. In contrast to the alteration in VLDL-TG secretion, neither apoB100 (Figure 5C) nor apoB48 (Figure 5D) secretion was different, suggesting that equivalent numbers of newly synthesized VLDL particles were secreted from both groups, but that these particles differ with respect to their lipid content. To determine whether increased LDL catabolism or clearance of TG-rich lipoproteins may also contribute to the decreased plasma lipids in *Ilrun*KO mice, we performed an *in vivo* LDL clearance study and oral fat tolerance test. As suggested by the plasma ^{125}I decay curve (Online Figure IIIF), LDL FCRs were similar between genotypes (Online Figure IIIG). No significant difference in postprandial dynamic plasma TG levels was noted between groups (Online Figure IIIH–I). These results suggest that ILRUN deficiency results in lower non-HDL-C by reducing hepatic production of VLDL, rather than by enhancing apoBLp clearance.

Loss of Ilrun results in impaired glucose tolerance.

Dyslipidemia, including low plasma HDL-C levels, is characteristic of a cluster of metabolic factors that increase the risk for cardiovascular disease, namely the metabolic syndrome[32]. Since impaired fasting glucose or type 2 diabetes is one of the defining components of metabolic syndrome, we also investigated the effect of *Ilrun* on whole-body glucose homeostasis. In spite of comparable blood glucose levels under *ad libitum* fed or overnight fasted conditions, we have consistently observed impaired glucose tolerance in chow-fed *Ilrun*KO vs. WT mice (Online Figure IVA–B). After an overnight fast and a challenge with intraperitoneal injection of sodium pyruvate, gluconeogenesis did not differ between groups (Online Figure IVC). Furthermore, whole-body insulin sensitivity as measured by an insulin tolerance test was also similar between genotypes (Online Figure IVD). *ILRUN* is expressed in human pancreatic islet cells, including insulin producing beta cells[33]. We found that ILRUN is specifically located in islets of pancreas in mice (Figure 1C). Therefore, we tested if glucose stimulated insulin secretion is attenuated in the absence of *Ilrun*. Intriguingly, while basal overnight fast plasma insulin levels were almost identical, insulin levels at 5 minutes after glucose injection were significantly lower in *Ilrun*KO vs. control mice (Online Figure IVE).

Mice were challenged with a high fat diet to further explore the impact of *Ilrun* on diet-induced obesity and glucose homeostasis under this condition. Body weight gain and weight of metabolic tissues were not different (Online Figure IVF–G). In agreement with findings from other cohorts, basal plasma cholesterol and PL levels were significantly decreased with *Ilrun* deletion. High fat diet consumption induced plasma lipid levels for both groups of mice, and the relative difference in plasma cholesterol and PL levels between genotypes remained. Increased plasma NEFA with diet feeding was observed as expected, but no significant difference between groups was detected (Online Figure IVH–J). Similar to observations in chow-fed mice, metabolic profiling uncovered impaired glucose tolerance without significant changes in steady state glucose, gluconeogenesis, or whole-body insulin sensitivity in *Ilrun*KO vs. WT mice (Online Figure IVK–N). Plasma insulin in control mice were similar to baseline levels after glucose stimulation for 30 or 60 minutes, whereas in *Ilrun*KO mice insulin at 60 minutes after glucose stimulation was significantly lower than baseline level (Online Figure IVO). Together, these data demonstrate that global deletion of *Ilrun* impairs glucose tolerance potentially by regulating glucose stimulated insulin secretion.

Ilrun deficiency alters the liver transcriptome profile and increases protein abundance of hepatic PPARα and RXRα.

To address the transcriptional effect of loss of *Ilrun* in liver, we examined expression of genes encoding proteins with key roles in lipoprotein and liver lipid metabolism. In chow-fed mice, while the majority of tested genes remained the same between genotypes (Online Figure V), we noted significant reductions in mRNAs of *Apoa1* and *Apoa4*, as well as some lipogenic genes *(Scd1* and *Fads1)*. Overall, these transcriptional changes did not result in a net change in steady state liver lipid accumulation in adult mice, as suggested by similar hepatic TG and TC contents in two genotypes (Online Figure VIA). After 14 wks of WTD consumption, liver lipid content was substantially increased in control mice but was significantly blunted in *Ilrun*KO mice, resulting in 19% lower TG and 25% lower TC levels in liver (Online Figure VIB). Examination of genes involved in different aspects of lipid metabolism revealed highly significantly reduced expression of *Apoa4*, a positive regulator of VLDL particle expansion[34], as well as modestly decreased expression of lipogenic genes, such as *Scd1*, *Fads1*, *Fads2* and *Elovl3* (Online Figure VC), which may have contributed to the liver lipid content change under conditions of dietary lipid overload.

To gain insights into the mechanisms by which hepatic ILRUN may impact lipoprotein metabolism, we explored transcriptome-wide profiles of the livers of chow-fed *Ilrun*KO compared with WT mice by gene expression microarray analysis. A total of 403 genes were differentially expressed (false discovery rate <10%, absolute fold change>1.5), among which 220 were up-regulated and 183 were down-regulated in *Ilrun*KO versus control livers (Figure 6A). As expected, *Ilrun* was the most significantly down-regulated gene (fold change=−22.7) (Online Figure VIIA). Functional analysis of differentially expressed genes by Ingenuity Pathway Analysis (IPA) identified lipid metabolism as the top biological function that was most significant to the molecules in the gene set. Gene ontology enrichment analysis with Reactome pathways also revealed significant enrichment of metabolism of lipids pathway, with metabolism and retinoid metabolism and transport being

the other two pathways on the list (Online Figure VIIB). Similar results were obtained with Gene ontology analysis of biological processes (Online Table II). Pathway analysis of the gene expression data showed that this altered gene set was enriched for genes downstream of multiple upstream regulator pathways, including known regulators of lipid metabolism, such as the top ranked peroxisome proliferator activated receptor α (PPARα). In addition, its binding partner retinoid × receptor alpha (RXRα) as well as the other two members of the PPAR family, PPARγ and PPARδ, were also highly ranked by this analysis (Figure 6B). In primary hepatocytes and livers, we tested expression of some top up- or down- regulated genes and genes revealed by pathway analysis. In addition to genes we identified earlier in liver through RT-PCR, we also confirmed upregulation of adipokine *Cfd*, lipid droplet associated proteins (*Plin4, Cidec, Cidea*), and retinoic acid-metabolizing enzyme *Cyp26a1*. Importantly, many of these gene expression changes normalized with AAV-mediated hepatic human *ILRUN* expression, suggesting a direct relationship between hepatic *Ilrun* gene dosage and transcription of these select genes (Online Figure V and VIIC).

Interestingly, analysis of liver lysates and primary hepatocytes both revealed increased PPARα protein levels in *Ilrun*KO relative to control mice, while *Ppara* transcript levels were not increased (Figure 6C–D). Moreover, hepatic *ILRUN* reconstitution in *Ilrun*KO mice reduced liver PPARα protein levels (Online Figure IIB). We also examined expression of RXRα, the heterodimer binding partner of PPARα. While whole liver RXRα expression did not differ significantly (Figure 6C and Online Figure IIB), markedly increased RXRα protein expression with no significant change in *Rxra* transcript levels was observed in *Ilrun*-deficient primary hepatocytes (Figure 6C–D). This discrepancy likely reflected the difference between whole liver vs. hepatocytes as RXRα is also abundantly expressed in other cell types in the liver[35]. These results suggest a post-transcriptional effect of *Ilrun* deletion on PPARα and RXRα protein turnover. We also measured mRNA expression of the other two members of the PPAR family, *PPARγ* and *PPARδ*, and overall found no difference in *PPARδ* but increased *PPARγ* mRNA expression (Online Figure V, VI and VIIIA). Whole liver protein analysis did not reveal a major effect of *Ilrun* deletion on PPARγ protein abundance (Online Figure IIB), but in primary hepatocyte a modest ~50% increase was detected (Online Figure VIIIA).

ILRUN binds to ubiquitinylated proteins including PPARα in a UBA-like domain dependent manner.

The UBA-like and NBR1-like structure motifs present in ILRUN suggest a potential role for ILRUN in binding ubiquitinylated proteins and modulating their turnover. To test if ILRUN indeed binds to ubiqutinylated proteins, we transfected HEK293T cells with V5-tagged WT (*ILRUN*-V5) or two *ILRUN* variants deleted for the conserved motifs within it (*ILRUN*-UBAmut-V5 and *ILRUN*-NBR1mut-V5) and treated cells with MG132, a potent proteasome inhibitor. The V5 pull-down fraction was blotted for ubiquitin and ubiquitin conjugates. Ubiquitinylated proteins were detectable in precipitates from cells overexpressing full-length or *ILRUN*-NBR1mut-V5, but not cells expressing *ILRUN*-UBAmut-V5, supporting interactions of ILRUN with ubiquitinylated proteins in a UBA-like domain dependent manner (Figure 7A).

To investigate the possibility that ILRUN physically interacts with PPARα and if so, which domain(s) might be required for the interaction, we transfected COS7 cells with V5-tagged WT (*ILRUN*-V5), or two variants deleted either for the UBA-like domain (*ILRUN*-UBAmut-V5) or the NBR1-like domain (*ILRUN*-NBR1mut-V5), in the presence or absence of PPARα (Figure 7B). Analysis of whole cell lysates confirmed expression of ILRUN and/or PPARα. Cell lysates were immunoprecipitated with V5 agarose affinity gel and the precipitates were blotted for V5 and PPARα. Successful immunoprecipitation was confirmed by the presence of V5 bands in ILRUN expressing groups. PPARα was detectable in the pull-down fraction from cells co-expressing PPARα with either full-length *ILRUN* or *ILRUN*-NBR1mut-V5, but not with those expressing *ILRUN*-UBAmut-V5, which is in support of interactions between ILRUN and PPARα that are dependent on the UBA-like domain of ILRUN. Given the crucial role for the UBA-like domain in mediating ILRUN binding to ubiquitinylated proteins, these results suggest that ILRUN regulates PPARα protein turnover. In additional co-immunoprecipitation studies, full length ILRUN was also found to interact with PPARγ1 and PPARγ2 (Online Figure VIIIB).

In accordance with the potential relationship of ILRUN with nuclear transcriptional regulators, immunocytochemistry revealed both diffuse and punctate staining of endogenous ILRUN in HuH-7 nuclei, in addition to weaker staining in the cytoplasm. In mouse livers overexpressing *ILRUN*, immunohistochemistry revealed the expression of ILRUN in a similar fashion (Figure 7C).

DISCUSSION

GWAS have identified many novel genetic loci associated with plasma lipid traits for which the causal genes and mechanisms are completely unknown, providing a major opportunity for new biological discovery. One of the early novel lipid loci was *C6ORF106*[5, 6, 14], an uncharacterized open reading frame which we have participated in renaming *ILRUN*. Here, using *Ilrun*KO mice, we establish a previously unrecognized role for hepatic ILRUN in post-translational regulation of PPARα and thus in lipid homeostasis, strongly supporting *ILRUN* as the gene causal of the human genetic association with plasma lipid traits at this locus.

One of the prominent observations in our study is decreased plasma HDL-C levels in *Ilrun*KO mice. Our kinetic studies of HDL in mice indicate that neither increased HDL catabolism nor increased selective uptake of cholesterol explain the lower HDL-C levels, pointing instead to reduced HDL production as the underlying mechanism. Indeed, analysis of *Ilrun*KO primary hepatocyte, whole liver, and plasma all revealed notable reductions in expression of apoA-I, a major HDL moiety that is critical for nascent HDL formation and plasma HDL-C homeostasis[29]. More importantly, reconstitution in chow-fed *Ilrun*KO liver with human *ILRUN* restored *Apoa1* transcript and protein levels to those similar to WT mice, consistent with an effect of hepatic ILRUN on *Apoa1* transcription and apoA-I protein production under this condition. *Ilrun* deficiency in WTD-fed mice resulted in remarkably lower liver and plasma apoA-I protein levels without significant changes in liver *Apoa1* transcript, suggesting potential additional post-transcriptional regulation of apoA-I by ILRUN that becomes evident in response to dietary lipid overload.

*Ilrun*KO mice also exhibited significantly lower levels of non-HDL-C, predominantly LDL-C, especially when mice were fed a high-fat, high-cholesterol diet. Expression of liver transcripts related to LDL catabolism was unchanged, and the fractional catabolic rate of ^{125}I-LDL apoB was unaltered, indicating that increased LDL clearance is not the cause of lower plasma LDL-C. Conversely, studies of VLDL production uncovered markedly reduced VLDL-TG secretion in *Ilrun*KO mice. In our survey of hepatic genes, we noted significant changes in genes governing multiple aspects of liver lipid homeostasis, including fatty acid transport (*Cd36)*, lipid storage (*Plin4, Cidec, Cidea*), lipogenesis (*Scd1*, *Fads1*, *Fads2* and *Elovl3*), and VLDL secretion (*Apoa4*). *Apoa4* has a suggested direct role in modulating apoBLp TG expansion, while these other differentially expressed genes have demonstrated roles in hepatic and/or plasma lipid metabolism[34, 36–42]. *Ilrun*KO livers had significantly reduced TG and TC accumulation in response to excess dietary fat and cholesterol (i.e. WTD) where they also secreted lipid poor VLDL particles. It is therefore reasonable to hypothesize based on the gene expression signature that altered hepatic intracellular lipid transport and metabolism, including decreased lipogenesis and VLDL particle expansion, may have at least partially contributed to the reduced VLDL-TG secretion in *Ilrun*KO mice.

We used global transcriptome profiling approach to address the question of how liver ILRUN mediates these observed metabolic changes. Pathway analysis revealed enrichment of genes downstream of several nuclear receptor pathways, in particular PPARα. Further comparison with an RNA-seq result from fenofibrate treated mice suggested that ILRUN deletion regulates some genes similarly to PPARα activation by fenofibrate, including reduced *Apoa4* and *Apoa1* expression (R. Soccio, unpublished observation). Adding to the concept of altered PPARα activity was our finding of significantly increased PPARα protein abundance in *Ilrun*-deficient livers and primary hepatocytes. PPARα, the molecular target for the fibrate class of drugs, has an important role in lipoprotein metabolism by influencing expression of select sets of genes[43]. Fibrates raise plasma HDL-C levels and positively upregulate *APOA1* expression in human hepatocytes[44]. However, the effect of PPARα activation on *Apoa1* in rodents is opposite to that in humans[45], which is proposed to be due to a 3 nucleotide difference in the promoter A site and subsequent species-specific regulation involving PPARα-dependent induction of a negative transcriptional regulator Rev-erbα[46]. Thus, in mice, synthetic PPARα agonist treatment reduces, while genetic PPARα deficiency increases plasma TC and HDL-C levels[46–48]. Overall, the reduced *Apoa1* transcription and lower plasma HDL-C in *Ilrun*KO mice on chow is consistent with HDL metabolism changes associated with PPARα activation as a result of post-translational regulation by ILRUN.

PPARα has also been shown to significantly impact VLDL production. In mice, activation of PPARα markedly reduces VLDL-TG production *in vivo*, whereas PPARα deletion is associated with increased liver VLDL-TG production[49–51]. The similarity of our finding with known effects of PPARα on VLDL-TG is consistent with the concept that hepatic ILRUN influences PPARα activity. The regulation of hepatic TG storage and VLDL production by PPARα is generally attributed to its role in fatty acid oxidation (FAO). However, the regulation of other genes and metabolic pathways by PPARα may also contribute to some degree, as multiple aspects of hepatic lipid metabolism are under control by PPARα[52], and the precise target genes responsible for the effect of PPARα on VLDL production remain to be fully elucidated[43]. Although we did not observe significant

differences in expression of select β-oxidation genes, the functional outcome of ILRUN deficiency on FAO and other hepatic metabolic pathways (e.g. de novo lipogenesis and VLDL particle expansion) has yet to be directly evaluated. Comprehensive future investigation of the impact of ILRUN on these pathways is in need to elucidate the molecular mechanism underlying reduced VLDL-TG production in *Ilrun*KO mice and its relationship to PPARα regulation by ILRUN.

Another novel finding from our study is impaired glucose tolerance associated with global *Ilrun* deficiency through metabolic profiling of mice on chow and HFD. There was no significant difference in steady state glucose levels, gluconeogenesis or whole-body insulin sensitivity between groups, whereas *in vivo* glucose stimulated insulin secretion appeared to be attenuated in *Ilrun*KO vs. WT mice and may be responsible for impaired glucose tolerance in these mice. Given the specific expression of ILRUN in pancreatic islets, defining the effect of pancreatic β cell ILRUN on insulin secretion and glucose homeostasis will provide the opportunity to delineate tissue specific role of ILRUN in glucose homeostasis as well as insights into the biological function of ILRUN.

A select set of PPARα target genes were differentially expressed as one would expect with PPARα activation. However, the expression of some canonical PPARα target genes were either unchanged or regulated in the opposite direction to PPARα activation, in the presence of increased total PPARα protein in *Ilrun*KO hepatocytes. It suggests a more nuanced regulation of PPARα activity by ILRUN or additional upstream regulators impacted by ILRUN deficiency. The former concept is supported by the several layers regulation of PPARs activity *in vivo*, including availability of endogenous ligands, signaling through binding partner RXRα, modulation of transcriptional cofactors, and accessibility to promotors of target genes. For example, reduced fatty acid desaturase activity may limit unsaturated fatty acid availability[43]. RXRα forms a permissive heterodimer with PPARα that allows for dual-ligand regulation[53]. Adding to the complexity is potential regulation of RXRα protein turnover by ILRUN as suggested by our study. In HeLa cells, ILRUN has been shown to not only modulate IRF3 binding to DNA but also protein abundance of the transcriptional co-activators P300 and cAMP-response element-binding protein-binding protein[18], suggesting potential multifaceted roles of ILRUN through protein-protein interaction. The latter concept is understandable considering crosstalk of lipid transcriptional regulators in the liver, such as other PPAR isoforms and Liver × receptor α that also dimerize with RXRα, and sterol regulatory binding proteins[54]. Intracellular lipid metabolism is tightly controlled to coordinate physiological processes. Gene regulation by dual or multiple upstream transcriptional regulators is common. Our study linking ILRUN and other members of the PPARs/RXRα signaling suggests ILRUN may play a broader role in the liver. It is therefore possible that part of the gene expression signature has contributions from additional transcriptional regulators.

The exact molecular mechanisms by which ILRUN modulates transcription of select genes in the liver remain less clear. The ILRUN protein is not predicted to have a DNA-binding domain, but our data demonstrate its ability to interact with nuclear transcription factors (i.e. PPARα and PPARγ). Importantly, the UBA-like domain, but not the NBR1-like domain, of ILRUN is essential in the case of ILRUN-PPARα interaction. The presence of the UBA

domain in many members of the UBA-like superfamily enables their binding to ubiquitinylated proteins and thus either positively or negatively regulate target protein turnover through different mechanisms[55]. We found ILRUN to be abundant in the nuclei of hepatocytes, in both diffuse staining and in concentrated punctate foci. It is worth noting that the ILRUN-containing nuclear punctate-like structure may be one of these defined nuclear bodies, steady-state membrane-less subnuclear organelles that are highly dynamically responsive to basic physiological processes[56], or a yet to be characterized type of nuclear body. As various nuclear bodies have been shown to sequester and modify proteins and mediate nuclear protein turnover[57], it is plausible to speculate that ILRUN binds to ubiquitinylated PPARα to regulate its turnover and accessibility to DNA via the distinct nuclear dynamic machinery. Beyond PPARα, whether ILRUN plays a broader role in hepatocytes by modulating transcriptional regulators through similar or different mechanisms merits detailed mechanistic studies in the future.

In conclusion, inspired by human genetic studies, we investigated the functional link between ILRUN and lipid metabolism. The present work in mice establishes hepatic ILRUN as a novel regulator of plasma HDL and apoBLp metabolism. Furthermore, we provide functional evidence that loss of hepatic ILRUN impairs plasma lipoprotein production, likely by modulating lipid-related transcriptional regulators, especially PPARα, and subsequent gene expression. This model of hepatic ILRUN function is possibly the underlying mechanism for the association of the *ILRUN* locus with plasma lipid traits. Future studies on the precise molecular mechanisms of liver ILRUN function may uncover new pathways in the regulation of lipid metabolism and point toward promising approaches for treatment of dyslipidemia and associated cardiovascular diseases.

Supplementary Material

Refer to Web version on PubMed Central for supplementary material.

ACKNOWLEDGMENTS

The authors gratefully acknowledge Texas A&M Institute for Genomic Medicine for providing the ES cells to generate the mice and the UC Davis KOMP Phenotyping Project for providing *Ilrun*KO mice by request. We thank the University of Pennsylvania Diabetes Research Center (DRC) for the use of the Functional Genomics Core for microarray analysis, the Histology and Gene Expression Core for assistance in tissue histology analysis, the Cell and Developmental Biology Microscopy Core for confocal microscopy, and the Preclinical Vector Core for providing gene vectors used in this study. We thank Aisha Wilson, Maosen Sun, Edwige Edouard, Debra Cromley, Kevin Trindade, Yi-An Ko, Donna Conlon, Xinyu Zhao, Junichiro Tohyama, Wen Lin, and Hye In Kim for technical assistance, Dawn Marchadier for project management, and Linda Carmichael and Stephanie DerOhannessian for additional administrative support. We gratefully acknowledge Dr Mitchell Lazar for providing PPARγ plasmids and helpful discussion, Drs Sean Armour, Salam Ibrahim, Jeff Billheimer, and John Tobias for helpful discussions regarding our data, many past and present members of the Rader lab for thoughtful discussions and suggestions.

SOURCES OF FUNDING

This work was supported by National Institutes of Health grants RC2 HL101864, R01 HL089309 (to D.J.R.), American Heart Association Postdoctoral Fellowship 15POST25160019 and Career Development Award 19CDA34630032 (to X.B.). The DRC Functional Genomics Core was supported by NIH P30-DK19525.

Nonstandard Abbreviations and Acronyms:

AAV	Adeno-Associated Virus
C6ORF106	Chromosome 6 Open Reading Frame 106
CAD	Coronary Artery Disease
FPLC	Fast Protein Liquid Chromatography
FAO	Fatty Acid Oxidation
FCR	Fractional Catabolic Rate
GWAS	Genome-wide Association Studies
HDL-C	High-density Lipoprotien-Cholesterol
HFD	High Fat Diet
ILRUN	Inflammation and Lipid Regulator with UBA-like and NBR1-like domains
LDL-C	Low-density Lipoprotein-Cholesterol
LPL	Lipoprotein Lipase
NBR1	Next to BRCA1 gene 1 protein
NEFA	Non-esterified Fatty Acid
PL	Phospholipid
PPARα	Peroxisome Proliferator Activated Receptor α
SNPs	Single Nucleotide Polymorphisms
SR-BI	Scavenger receptor class B1
TC	Total Cholesterol
TBG	Thyroxine Binding Globulin
UBA	Ubiquitin Associated Domain
VLDL	Very-low density lipoprotein
WT	Wild Type
WTD	Western Type Diet

REFERENCES

1. Burkhardt R, Toh SA, Lagor WR, et al. Trib1 is a lipid- and myocardial infarction-associated gene that regulates hepatic lipogenesis and vldl production in mice. J Clin Invest. 2010;120:4410–4414 [PubMed: 21084752]

2. Bauer RC, Sasaki M, Cohen DM, Cui J, Smith MA, Yenilmez BO, Steger DJ, Rader DJ. Tribbles-1 regulates hepatic lipogenesis through posttranscriptional regulation of c/ebpalpha. J Clin Invest. 2015;125:3809–3818 [PubMed: 26348894]

3. Hsieh J, Koseki M, Molusky MM, et al. Ttc39b deficiency stabilizes lxr reducing both atherosclerosis and steatohepatitis. Nature. 2016;535:303–307 [PubMed: 27383786]

4. Musunuru K, Strong A, Frank-Kamenetsky M, et al. From noncoding variant to phenotype via sort1 at the 1p13 cholesterol locus. Nature. 2010;466:714–719 [PubMed: 20686566]

5. Teslovich TM, Musunuru K, Smith AV, et al. Biological, clinical and population relevance of 95 loci for blood lipids. Nature. 2010;466:707–713 [PubMed: 20686565]

6. Willer CJ, Schmidt EM, Sengupta S, et al. Discovery and refinement of loci associated with lipid levels. Nat Genet. 2013;45:1274–1283 [PubMed: 24097068]

7. Willer CJ, Sanna S, Jackson AU, et al. Newly identified loci that influence lipid concentrations and risk of coronary artery disease. Nat Genet. 2008;40:161–169 [PubMed: 18193043]

8. Spracklen CN, Chen P, Kim YJ, et al. Association analyses of east asian individuals and trans-ancestry analyses with european individuals reveal new loci associated with cholesterol and triglyceride levels. Hum Mol Genet. 2017;26:1770–1784 [PubMed: 28334899]

9. Davis JP, Huyghe JR, Locke AE, et al. Common, low-frequency, and rare genetic variants associated with lipoprotein subclasses and triglyceride measures in finnish men from the metsim study. PLoS Genet. 2017;13:e1007079 [PubMed: 29084231]

10. Below JE, Parra EJ, Gamazon ER, et al. Meta-analysis of lipid-traits in hispanics identifies novel loci, population-specific effects, and tissue-specific enrichment of eqtls. Sci Rep. 2016;6:19429 [PubMed: 26780889]

11. Hoffmann TJ, Theusch E, Haldar T, et al. A large electronic-health-record-based genome-wide study of serum lipids. Nat Genet. 2018;50:401–413 [PubMed: 29507422]

12. Lu X, Peloso GM, Liu DJ, et al. Exome chip meta-analysis identifies novel loci and east asian-specific coding variants that contribute to lipid levels and coronary artery disease. Nat Genet. 2017;49:1722–1730 [PubMed: 29083407]

13. Liu DJ, Peloso GM, Yu H, et al. Exome-wide association study of plasma lipids in >300,000 individuals. Nat Genet. 2017;49:1758–1766 [PubMed: 29083408]

14. Klarin D, Damrauer SM, Cho K, et al. Genetics of blood lipids among ~300,000 multi-ethnic participants of the million veteran program. Nat Genet. 2018

15. Consortium CAD, Deloukas P, Kanoni S, et al. Large-scale association analysis identifies new risk loci for coronary artery disease. Nat Genet. 2013;45:25–33 [PubMed: 23202125]

16. Nikpay M, Goel A, Won HH, et al. A comprehensive 1,000 genomes-based genome-wide association meta-analysis of coronary artery disease. Nat Genet. 2015;47:1121–1130 [PubMed: 26343387]

17. van der Harst P, Verweij N. Identification of 64 novel genetic loci provides an expanded view on the genetic architecture of coronary artery disease. Circ Res. 2018;122:433–443 [PubMed: 29212778]

18. Ambrose RL, Liu YC, Adams TE, Bean AGD, Stewart CR. C6orf106 is a novel inhibitor of the interferon-regulatory factor 3-dependent innate antiviral response. J Biol Chem. 2018;293:10561–10573 [PubMed: 29802199]

19. Ambrose RL, Brice AM, Caputo AT, Alexander MR, Tribolet L, Liu YC, Adams TE, Bean AGD, Stewart CR. Molecular characterisation of ilrun, a novel inhibitor of proinflammatory and antimicrobial cytokines. Heliyon. 2020;6:e04115 [PubMed: 32518853]

20. Marchler-Bauer A, Derbyshire MK, Gonzales NR, et al. Cdd: Ncbi's conserved domain database. Nucleic Acids Res. 2015;43:D222–226 [PubMed: 25414356]

21. Marchler-Bauer A, Bo Y, Han L, et al. Cdd/sparcle: Functional classification of proteins via subfamily domain architectures. Nucleic Acids Res. 2017;45:D200–D203 [PubMed: 27899674]

22. Hofmann K, Bucher P. The uba domain: A sequence motif present in multiple enzyme classes of the ubiquitination pathway. Trends Biochem Sci. 1996;21:172–173 [PubMed: 8871400]

23. Dikic I, Wakatsuki S, Walters KJ. Ubiquitin-binding domains - from structures to functions. Nat Rev Mol Cell Biol. 2009;10:659–671 [PubMed: 19773779]

24. Marchbank K, Waters S, Roberts RG, Solomon E, Whitehouse CA. Map1b interaction with the fw domain of the autophagic receptor nbr1 facilitates its association to the microtubule network. Int J Cell Biol. 2012;2012:208014 [PubMed: 22654911]

25. Kraft C, Peter M, Hofmann K. Selective autophagy: Ubiquitin-mediated recognition and beyond. Nat Cell Biol. 2010;12:836–841 [PubMed: 20811356]

26. Johansen T, Lamark T. Selective autophagy mediated by autophagic adapter proteins. Autophagy. 2011;7:279–296 [PubMed: 21189453]

27. Coordinators NR. Database resources of the national center for biotechnology information. Nucleic Acids Res. 2017

28. Consortium GT, Laboratory DA, Coordinating Center-Analysis Working G, Genetic effects on gene expression across human tissues. Nature. 2017;550:204–213 [PubMed: 29022597]

29. Luo J, Yang H, Song BL. Mechanisms and regulation of cholesterol homeostasis. Nat Rev Mol Cell Biol. 2020;21:225–245 [PubMed: 31848472]

30. Stylianou IM, Svenson KL, VanOrman SK, Langle Y, Millar JS, Paigen B, Rader DJ. Novel enu-induced point mutation in scavenger receptor class b, member 1, results in liver specific loss of scarb1 protein. PLoS One. 2009;4:e6521 [PubMed: 19654867]

31. Khoo JC, Pittman RC, Rubin EM. Selective uptake of hdl cholesteryl esters is active in transgenic mice expressing human apolipoprotein a-i. J Lipid Res. 1995;36:593–600 [PubMed: 7775870]

32. Ginsberg HN, Zhang YL, Hernandez-Ono A. Metabolic syndrome: Focus on dyslipidemia. Obesity (Silver Spring). 2006;14 Suppl 1:41S–49S [PubMed: 16642962]

33. Segerstolpe A, Palasantza A, Eliasson P, et al. Single-cell transcriptome profiling of human pancreatic islets in health and type 2 diabetes. Cell Metab. 2016;24:593–607 [PubMed: 27667667]

34. VerHague MA, Cheng D, Weinberg RB, Shelness GS. Apolipoprotein a-iv expression in mouse liver enhances triglyceride secretion and reduces hepatic lipid content by promoting very low density lipoprotein particle expansion. Arterioscler Thromb Vasc Biol. 2013;33:2501–2508 [PubMed: 24030551]

35. MacParland SA, Liu JC, Ma XZ, et al. Single cell rna sequencing of human liver reveals distinct intrahepatic macrophage populations. Nat Commun. 2018;9:4383 [PubMed: 30348985]

36. Brown JM, Rudel LL. Stearoyl-coenzyme a desaturase 1 inhibition and the metabolic syndrome: Considerations for future drug discovery. Curr Opin Lipidol. 2010;21:192–197 [PubMed: 20216310]

37. Zadravec D, Brolinson A, Fisher RM, et al. Ablation of the very-long-chain fatty acid elongase elovl3 in mice leads to constrained lipid storage and resistance to diet-induced obesity. FASEB J. 2010;24:4366–4377 [PubMed: 20605947]

38. Jump DB. Fatty acid regulation of hepatic lipid metabolism. Curr Opin Clin Nutr Metab Care. 2011;14:115–120 [PubMed: 21178610]

39. Gromovsky AD, Schugar RC, Brown AL, et al. Delta-5 fatty acid desaturase fads1 impacts metabolic disease by balancing proinflammatory and proresolving lipid mediators. Arterioscler Thromb Vasc Biol. 2018;38:218–231 [PubMed: 29074585]

40. Koonen DP, Jacobs RL, Febbraio M, Young ME, Soltys CL, Ong H, Vance DE, Dyck JR. Increased hepatic cd36 expression contributes to dyslipidemia associated with diet-induced obesity. Diabetes. 2007;56:2863–2871 [PubMed: 17728375]

41. Wilson CG, Tran JL, Erion DM, Vera NB, Febbraio M, Weiss EJ. Hepatocyte-specific disruption of cd36 attenuates fatty liver and improves insulin sensitivity in hfd-fed mice. Endocrinology. 2016;157:570–585 [PubMed: 26650570]

42. Carr RM, Ahima RS. Pathophysiology of lipid droplet proteins in liver diseases. Exp Cell Res. 2016;340:187–192 [PubMed: 26515554]

43. Rakhshandehroo M, Knoch B, Muller M, Kersten S. Peroxisome proliferator-activated receptor alpha target genes. PPAR Res. 2010;2010

44. Berthou L, Duverger N, Emmanuel F, et al. Opposite regulation of human versus mouse apolipoprotein a-i by fibrates in human apolipoprotein a-i transgenic mice. J Clin Invest. 1996;97:2408–2416 [PubMed: 8647932]

45. Vu-Dac N, Chopin-Delannoy S, Gervois P, Bonnelye E, Martin G, Fruchart JC, Laudet V, Staels B. The nuclear receptors peroxisome proliferator-activated receptor alpha and rev-erbalpha mediate

the species-specific regulation of apolipoprotein a-i expression by fibrates. J Biol Chem. 1998;273:25713–25720 [PubMed: 9748239]

46. Staels B, van Tol A, Andreu T, Auwerx J. Fibrates influence the expression of genes involved in lipoprotein metabolism in a tissue-selective manner in the rat. Arterioscler Thromb. 1992;12:286–294 [PubMed: 1547188]
47. Peters JM, Hennuyer N, Staels B, Fruchart JC, Fievet C, Gonzalez FJ, Auwerx J. Alterations in lipoprotein metabolism in peroxisome proliferator-activated receptor alpha-deficient mice. J Biol Chem. 1997;272:27307–27312 [PubMed: 9341179]
48. Montagner A, Polizzi A, Fouche E, et al. Liver pparalpha is crucial for whole-body fatty acid homeostasis and is protective against nafld. Gut. 2016;65:1202–1214 [PubMed: 26838599]
49. Kersten S Peroxisome proliferator activated receptors and lipoprotein metabolism. PPAR Res. 2008;2008:132960 [PubMed: 18288277]
50. Linden D, Alsterholm M, Wennbo H, Oscarsson J. Pparalpha deficiency increases secretion and serum levels of apolipoprotein b-containing lipoproteins. J Lipid Res. 2001;42:1831–1840 [PubMed: 11714852]
51. Tordjman K, Bernal-Mizrachi C, Zemany L, et al. Pparalpha deficiency reduces insulin resistance and atherosclerosis in apoe-null mice. J Clin Invest. 2001;107:1025–1034 [PubMed: 11306606]
52. Kersten S Integrated physiology and systems biology of pparalpha. Mol Metab. 2014;3:354–371 [PubMed: 24944896]
53. Evans RM, Mangelsdorf DJ. Nuclear receptors, rxr, and the big bang. Cell. 2014;157:255–266 [PubMed: 24679540]
54. Boergesen M, Pedersen TA, Gross B, et al. Genome-wide profiling of liver × receptor, retinoid × receptor, and peroxisome proliferator-activated receptor alpha in mouse liver reveals extensive sharing of binding sites. Mol Cell Biol. 2012;32:852–867 [PubMed: 22158963]
55. Su V, Lau AF. Ubiquitin-like and ubiquitin-associated domain proteins: Significance in proteasomal degradation. Cell Mol Life Sci. 2009;66:2819–2833 [PubMed: 19468686]
56. Mao YS, Zhang B, Spector DL. Biogenesis and function of nuclear bodies. Trends Genet. 2011;27:295–306 [PubMed: 21680045]
57. Zimber A, Nguyen QD, Gespach C. Nuclear bodies and compartments: Functional roles and cellular signalling in health and disease. Cell Signal. 2004;16:1085–1104 [PubMed: 15240004]

NOVELTY AND SIGNIFICANCE

What Is Known?

- Dyslipidemia is a key risk factor for atherosclerotic cardiovascular disease (CVD).
- The residual CVD risk requires exploration of new players in lipid metabolism and CVD development.
- Multiple variants near the *ILRUN* gene at human chromosome 6p21 are significantly associated with plasma lipid traits and coronary artery disease risk in genome-wide association studies.

What New Information Does This Article Contribute?

- *Ilrun* regulates plasma lipoprotein metabolism.
- Loss of *Ilrun* lowers plasma high density lipoprotein cholesterol (HDL-C) levels by decreasing hepatic apolipoprotein-AI expression and HDL production.
- Loss of *Ilrun* reduces plasma non-HDL-C levels by producing relatively lipid-poor very low density lipoprotein particles.
- ILRUN interacts with nuclear receptor PPARα via its UBA-like domain and regulates PPARα protein homeostasis.
- *ILRUN* is likely responsible for the association of genetic variants with lipid traits at the human 6p21 locus.

Despite successful current therapies, the large remaining CVD burden necessitates the search for additional pathways regulating its risk factors, including lipid regulators. Our study identifies ILRUN as a completely novel regulator of lipid and lipoprotein metabolism that promotes hepatic lipoprotein production. Better understanding of liver ILRUN biology may provide insights into approaches for treatment of dyslipidemia and CVD. These findings further support the concept that common population level natural genetic variation with small effect size are effective in revealing pathways and targets with biological and clinical importance.

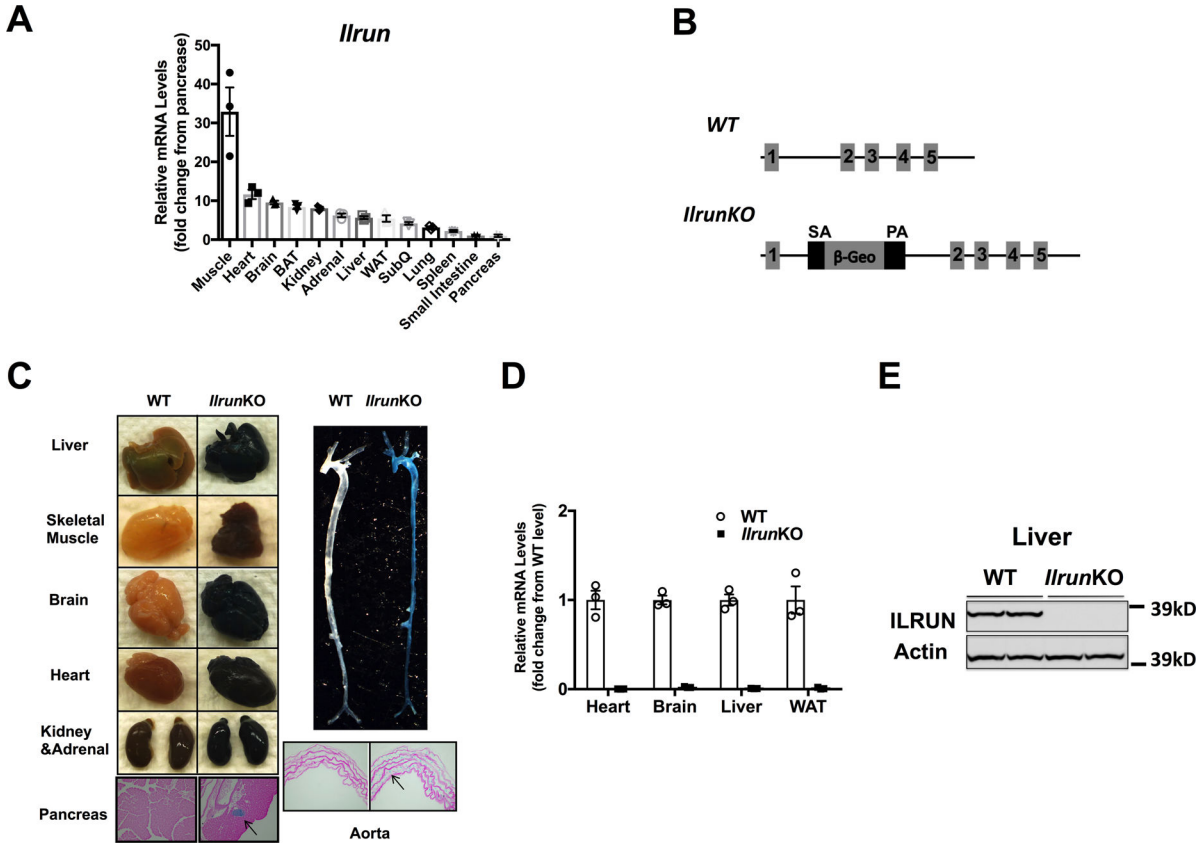

Figure 1. *Ilrun* expression and *Ilrun* whole body knockout mice.

A, Relative *Ilrun* mRNA expression across different tissues (fold change from pancreas) in male C57BL/6 mice was determined by RT-PCR. n=3/group. **B,** Targeting strategy for generation of *Ilrun*KO mice. **C,** Multiple tissues of female WT (left) and *Ilrun*KO (right) mice were stained with X-gal. Images of representative stained tissues and cross sections (light eosin) are shown. Scale bars represent 50μm. n=4/group. Deletion of *Ilrun* was validated by (**D**) RT-PCR (n=3/group) and (**E**) western blot. Results from representative tissues are shown. Data are shown as the mean ± SEM. Results in D were compared between genotypes by Mann-Whitney test.

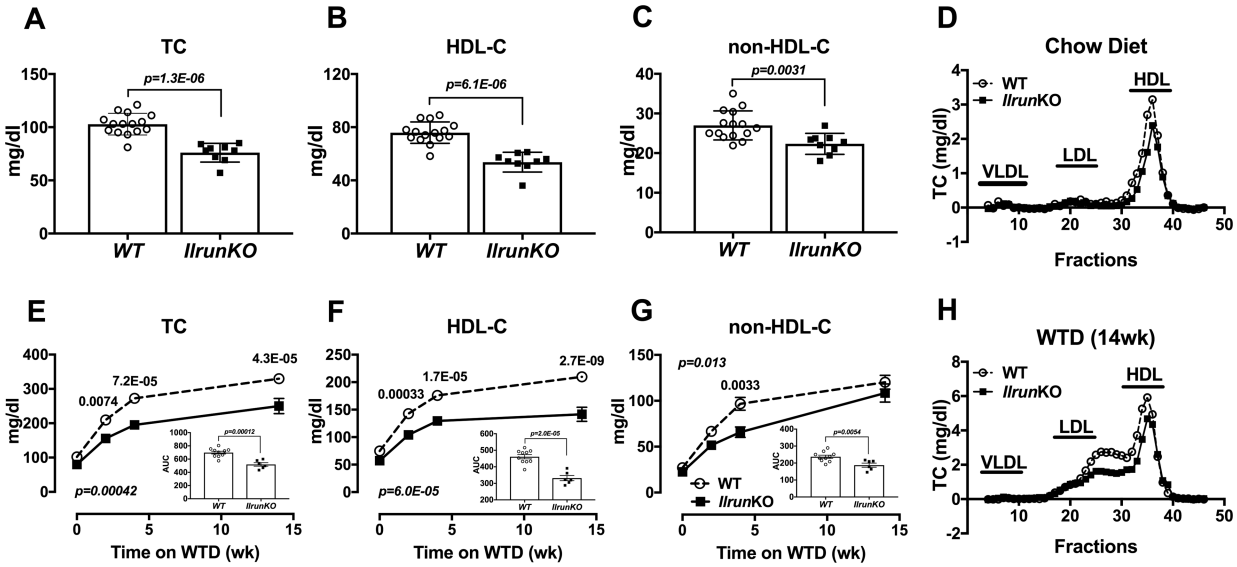

Figure 2. Deletion of *Ilrun* decreases plasma cholesterol levels in mice.

Four-hour fasted plasma from chow-fed male control (n=15) and *Ilrun*KO (n=9) mice were collected, plasma (**A**) TC and (**B**) HDL-C levels were measured. **C,** Non-HDL-C was calculated by subtracting HDL-C from TC. **D,** FPLC analysis of pooled plasma from each genotype. WT control (n=10) and *Ilrun*KO (n=6) mice were switched from chow diet to WTD for 14wk. Time course plasma (**E**) TC, (**F**) HCL-C and (**G**) non-HDL-C were determined. Pooled plasma from these mice were fractionated by FPLC (**H**). Data are shown as the mean ± SEM. Results in A, C, and E-G (area under the curve) were analyzed by Student's t test. Results in B were analyzed by Mann-Whitney test. Results in E-G were also compared with two-way ANOVA with Sidak's multiple comparison test. P values indicate comparisons between genotypes.

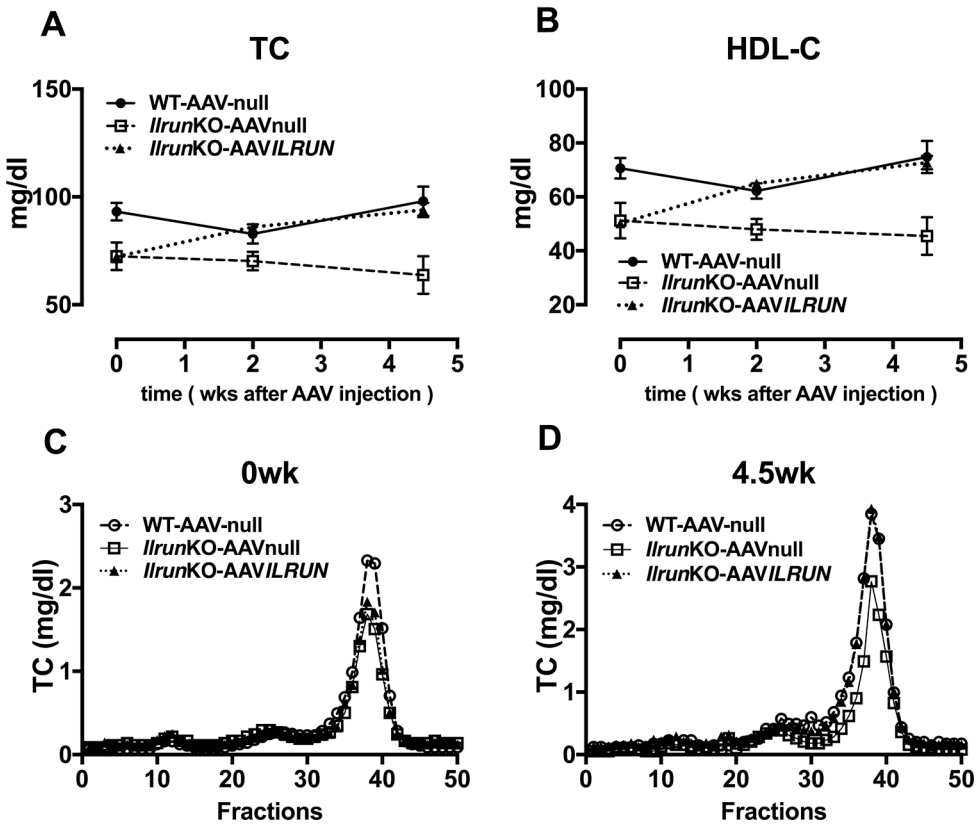

Figure 3. Reconstitution of *ILRUN* in livers of *Ilrun*KO mice restores plasma lipids to WT levels.

Male mice on chow diet were i.p. injected with AAV-null or AAV-*ILRUN* (WT-AAV-null n=5, *Ilrun*KO-AAVnull and *Ilrun*KO-AAV*ILRUN* n=4/group). Plasma lipid levels were monitored before (0wk), 2wk and 4.5wk after AAV injection. Plasma TC (**A**) and HDL-C (**B**) levels were measured. Pooled plasma from groups were fractionated by FPLC and TC at (**C**) baseline and (**D**) 4.5 wk after AAV injection were measured by enzymatic assays. Data are shown as the mean ± SEM.

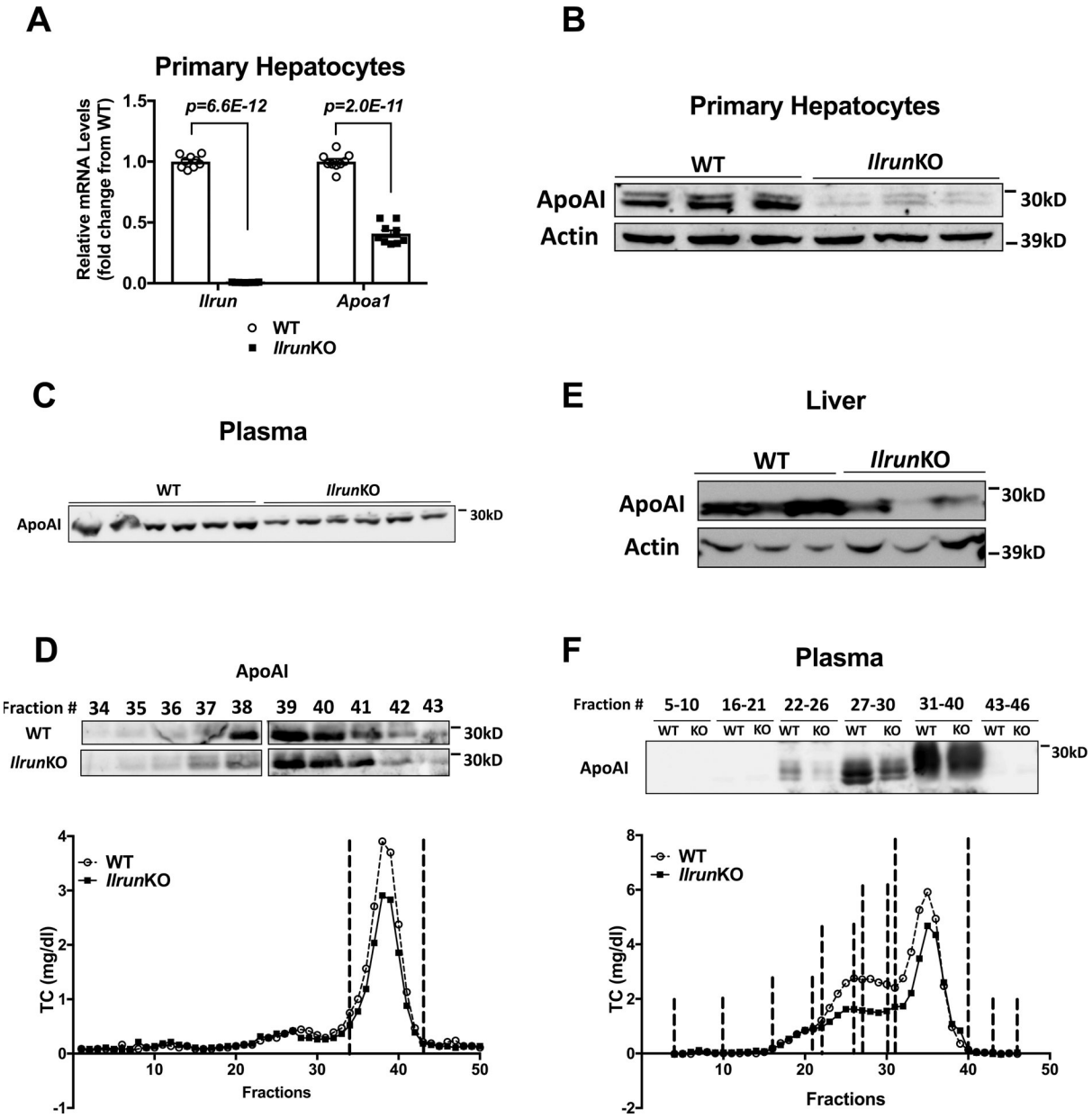

Figure 4. *Ilrun* deficiency reduces liver and plasma apoA-I levels.

Primary hepatocytes from chow-fed male mice were isolated for (**A**) mRNA (n=9/group) and (**B**) apoA-I protein analysis (n=3/group). **C,** ApoA-I levels in whole plasma (n=6/group) and (**D**) HDL fractions of male mice on chow diet (n=8/pool) were examined by western blot. ApoA-I expression in (**E**) liver and (**F**) FPLC fractions of pooled plasma from WTD-fed male mice were compared by western blot. n=6/group. Data are shown as the mean ± SEM. Results in A were analyzed by Student's t test with (*Ilrun*) or without (*Apoa1*) Welch's correction.

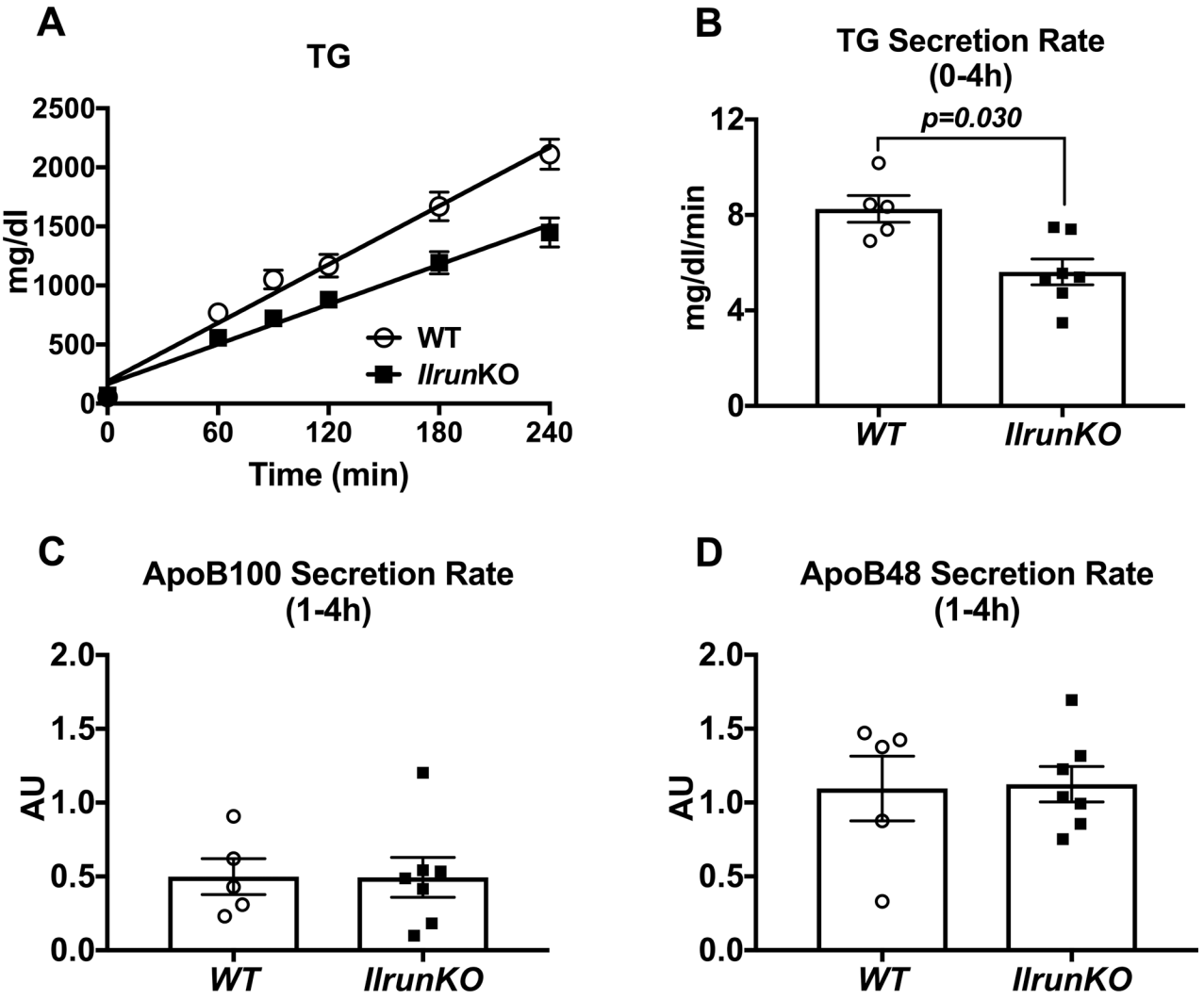

Figure 5. Deletion of *Ilrun* reduces VLDL-TG secretion rate.

Poloxamer 407 and ^{35}S-Methionine/Cysteine were i.v. injected into WTD-fed 4h-fasted male control (n=5) and *Ilrun*KO (n=7) mice. **A,** Plasma TG levels before and after injection were measured by enzymatic assays and the line of best fit was determined by linear regression analysis. **B,** TG secretion rate was calculated based on the slope of TG accumulation curve. Plasma samples from different time points were fractionated by SDS-PAGE and secretion rate of newly synthesized (**C**) apoB100 and (**D**) apoB48 were quantified by autoradiography. Data are shown as the mean ± SEM. Results in B-D were compared by Mann-Whitney test. P values indicate comparisons between genotypes.

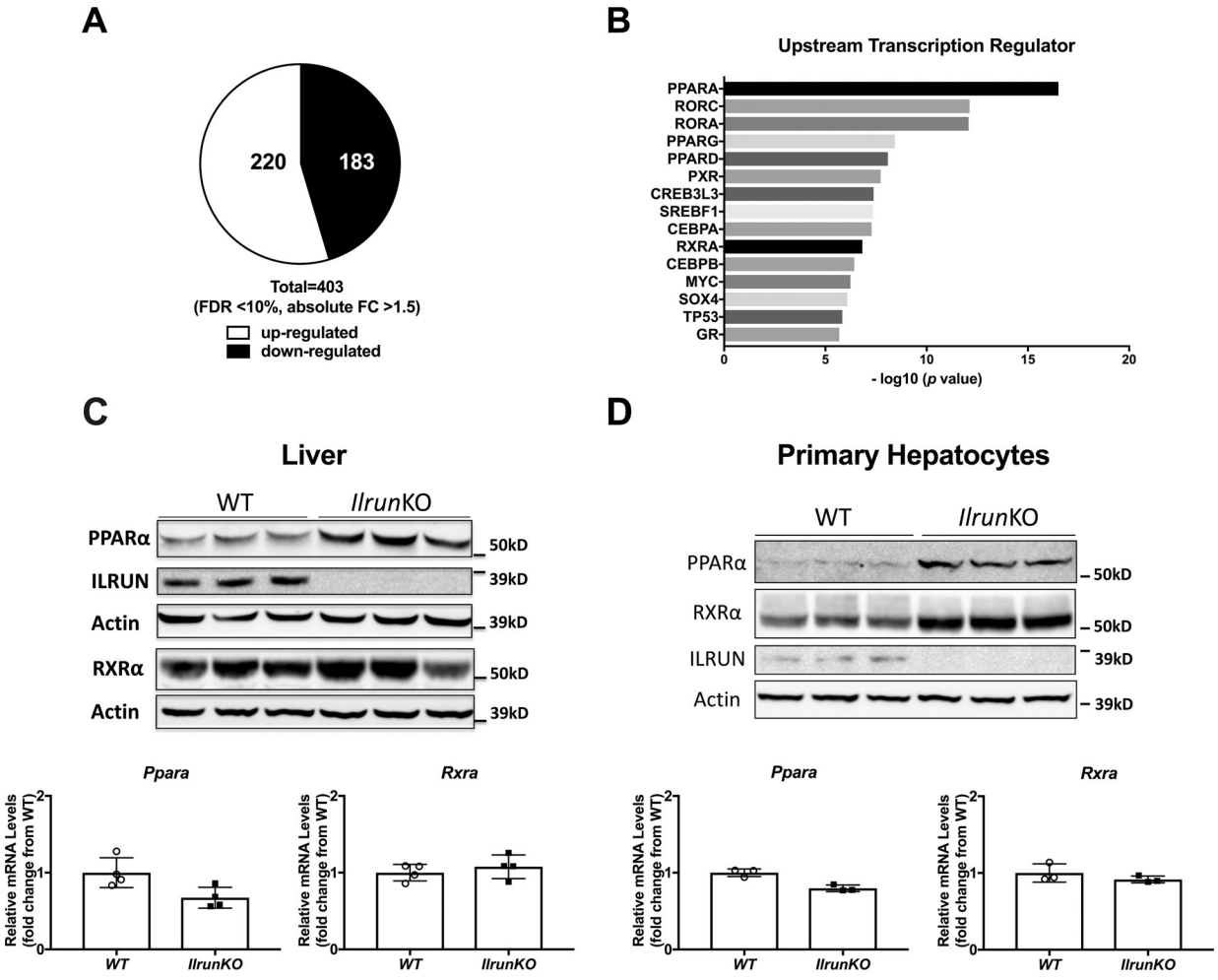

Figure 6. *Ilrun* deficiency alters liver transcriptome profiles and increases hepatic PPARα/RXRα protein levels.

Livers from chow-fed male *Ilrun*KO and WT mice were used for microarray analysis (n=4/group). **A,** Summary of up and down regulated genes at the cut-off of FDR<10% and absolute FC>1.5. **B,** Ingenuity pathway analysis was performed to predict upstream transcriptional regulators. Total PPARα and RXRα protein (top) and mRNA expression (bottom) in (**C**) livers (n=4/group) and (**D**) primary hepatocytes from chow-fed mice (n=3/group). Representative western blot images are from one of the experiments and reflect typical expression pattern between genotypes for proteins of interest. Data are shown as the mean ± SEM. RT-PCR results in C-D were analyzed by Mann-Whitney test.

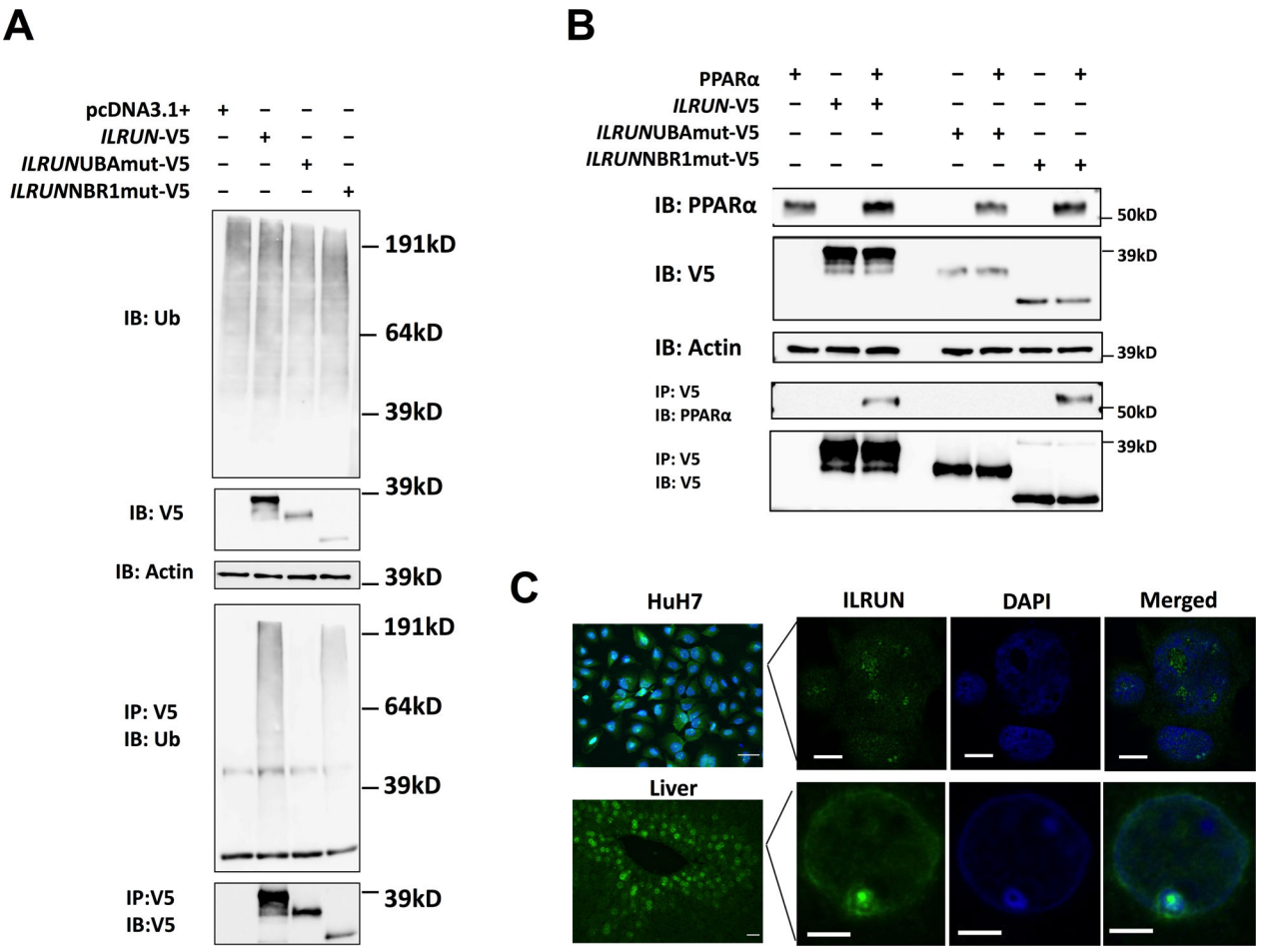

Figure 7. ILRUN binds to ubiquitinated proteins and PPARα.

A, Binding of full length or mutant forms of ILRUN to ubiquitinylated proteins was examined. **B,** Co-immunoprecipitation of PPARα and different forms of ILRUN followed by western blot analysis. **C,** Representative images depicting features typical of ILRUN stained HuH7 cells and livers using fluorescence microscope with a 20x objective lens (left) and confocal microscopy (right) are shown. Scale bars represent 50μm (left), 10μm (HuH7 confocal), and 5μm (liver confocal) respectively.